Observational Study

Medicine®

OPEN

# Initial experience with intensity distribution analysis of hemodynamic parameters in the thoracic aorta using four-dimensional magnetic resonance imaging

## A comparison between groups with different ejection fractions

Takamasa Nishimura, MD*, Eijun Sueyoshi, MD, Hirofumi Koike, MD, Masataka Uetani, MD

**Abstract**

The purpose of this study was to investigate whether there were significant differences in the intensity distributions of thoracic aorta hemodynamic parameters between groups with different ejection fractions (EF) using four-dimensional flow magnetic resonance imaging and to investigate the relationships between each parameter.

A total of 26 patients, 13 each with EF of >60% and <30%, underwent cardiac four-dimensional flow magnetic resonance imaging (EF >60%: mean age: 54 ± 11.6 years, EF <30%: mean age: 49.2 ± 17.2 years). The thoracic aorta was divided into the proximal and distal ascending aorta (AAo), aortic arch, and the proximal and distal descending aorta, and each section was further divided into the anterior wall, posterior wall, lesser curvature, and greater curvature. The intensity distributions of wall shear stress (WSS), energy loss (EL), and vorticity (Vort) (hemodynamic parameters) and the concordance rates between these distributions were analyzed.

The concordance rate between the intensity distributions of EL and Vort was high. Only the intensity distributions of EL and Vort in the distal AAo differed significantly between the groups ($P < .001$). In the EF >60% group, these intensity distributions showed higher values in the greater curvature of the AAo, whereas in the EF <30% group higher values were seen in the lesser curvature of the AAo.

Although there was no significant intergroup difference in the WSS intensity distribution, in the EF <30% group the WSS intensity distribution tended to exhibit higher values in the lesser curvature of the distal AAo, and the WSS intensity distribution values for the greater curvature tended to gradually increase from the arch to the proximal descending aorta.

The only significant differences between the EF groups were found in the intensity distributions of EL and Vort in the distal AAo. This suggests that the distributions of atherosclerosis may be EF-dependent.

**Abbreviations:** 4D flow MRI = four-dimensional flow magnetic resonance imaging, AAo = ascending aorta, BAV = bicuspid aortic valve, DAo = descending aorta, EF = ejection fraction, EL = energy loss, Vort = vorticity, WSS = wall shear stress.

**Keywords:** energy loss, four-dimensional flow magnetic resonance imaging, thoracic aorta, vorticity, wall shear stress

## 1. Introduction

Four-dimensional flow magnetic resonance imaging (4D flow MRI) can visualize blood flow in 4 dimensions by dividing it into numerous particles, tracking the motion of each particle, and connecting the velocity vectors of the particles at a given time. 4D flow MRI can be used to visualize and measure various hemodynamic parameters, such as wall shear stress (WSS), energy loss (EL), and vorticity (Vort). It is useful for studying

*Editor: Roxana Covali.*

*This study was supported by JSPS KAKENHI Grant Number 21K07733.*

*All procedures performed in studies involving human participants were in accordance with the ethical standards of the institutional and/or national research committee and with the 1964 Helsinki declaration and its later amendments or comparable ethical standards.*

*Our institutional review board approved this study, and the need for written informed consent was waived because this was a retrospective study.*

*The authors have no conflicts of interests to disclose.*

*Data sharing not applicable to this article as no datasets were generated or analyzed during the current study.*

*Department of Radiological Sciences, Graduate School of Biomedical Sciences, Nagasaki University, Nagasaki, Japan.*

** Correspondence: Takamasa Nishimura, Department of Radiological Sciences, Graduate School of Biomedical Sciences, Nagasaki University, 1-7-1 Sakamoto, Nagasaki 852-8501, Japan (e-mail: bb55320028@ms.nagasaki-u.ac.jp).*



*How to cite this article: Nishimura T, Sueyoshi E, Koike H, Uetani M. Initial experience with intensity distribution analysis of hemodynamic parameters in the thoracic aorta using four-dimensional magnetic resonance imaging: a comparison between groups with different ejection fractions. Medicine 2022;101:2(e28563).*

*Received: 19 August 2021 / Received in final form: 17 December 2021 / Accepted: 21 December 2021*

*http://dx.doi.org/10.1097/MD.0000000000028563*

diseases in which hemodynamics play a major role, such as cardiomyopathy, valvular disease, aortic disease, and pulmonary vascular disease.

WSS is the force generated by blood flow rubbing against the vascular intima. Previous studies have shown that low WSS is associated with the development of atherosclerosis,[1] and high WSS is associated with plaque failure.[2]

EL is a numerical indicator of the energy efficiency within a region of interest, and a high EL results in an increased cardiac load. It has attracted attention as an indicator for predicting cardiac load in valvular disease, cardiomyopathy, and congenital heart disease.[3]

Vort is an index that quantifies the strength of the swirl of the velocity vector. High Vort values may increase the pressure or stress on local blood vessel walls, promoting aneurysm growth, and may also alter local vascular protective mechanisms, leading to a reduction in WSS.[4,5] In other words, Vort is indirectly involved in the development of atherosclerosis.

The ejection fraction (EF) is commonly used as an index of cardiac function. It usually refers to the EF of the left ventricle, which is the ratio of left ventricular stroke volume to left ventricular end-diastolic volume. According to the American Society of Echocardiography and the European Association of Cardiovascular Imaging guideline, the normal EF is 63% ± 5%, and less than 30 is defined as severely abnormal.[6] However, the EF is only a ratio and does not directly relate to the actual volume of blood flow. The intensity distributions of hemodynamic parameters are expected to change with the volume and velocity of blood flow. It is also expected that the intensity distributions of these parameters will differ between patients with normal and decreased EF. However, no previous studies have examined such differences using 4D flow MRI.

The purpose of this study was to investigate whether the intensity distributions of hemodynamic parameters in the thoracic aorta differ between groups with different EF using 4D flow MRI and to examine the relationships between each hemodynamic parameter.

## 2. Methods

### 2.1. Study population

Our institutional review board approved this study, and the need for written informed consent was waived because this was a retrospective study.

From April 2019 to September 2020, 85 patients underwent cardiac contrast-enhanced MRI to investigate cardiomyopathy or cardiac dysfunction. Since 4D flow analysis is performed at the same time as cardiac MRI in our hospital, 85 patients also underwent 4D flow MRI. Of these, EF of >60% and <30% were found in 18 and 23 patients, respectively. The exclusion criteria included patients with aortic valve disease, such as aortic stenosis or regurgitation; patients with bicuspid aortic valve (BAV); patients who had undergone aortic valve or thoracic aorta surgery. It has been reported that patients with aortic valve stenosis or BAV exhibit significantly different WSS intensity distributions in the ascending aorta (AAo) from patients with normal tricuspid valves.[7,8] Therefore, it was expected that in patients with these conditions the WSS intensity distribution would be affected regardless of the EF; hence, we excluded cases involving these diseases. Among the patients who underwent 4D flow MRI, aortic valve disease was present in 4 of those with EF of >60% and 7 of those with EF of <30%, and none had BAV or history of aortic surgery. In addition, there were 1 and 3 patients with EF of >60% and EF <30%, respectively, who could not be analyzed due to inadequate phase imaging. A total of 26 patients were included in the final study, 13 each with EF of >60% and <30% (Fig. 1).

The patients' background data are shown in Table 1. The EF <30% group contained significantly more males and had a higher mean heart rate. However, there was no significant difference in the stroke volume index or cardiac output index between the 2 groups.

According to cardiac MRI, there were 9 patients with suspected dilated cardiomyopathy, 8 with suspected hypertrophic cardiomyopathy, and 2 with suspected amyloidosis; however, there were no obvious findings in the aorta itself.

### 2.2. Data acquisition and analysis

All patients were scanned using a 3.0 T MRI scanner (Magnetom Vida, Siemens Healthcare, Germany). The scanning parameters were as follows: repetition time/echo time/flip angle = 42.64 ms/2.99 ms/15 deg, voxel resolution = 0.9 × 0.9 × 4.0 mm, bandwidth = 1532 Hz/Px, velocity encoding (venc) = 150 cm/s, scan time = approx. 10 min (with compressed sensing).

All images were taken under free-breathing conditions using gadolinium-based contrast agents.

The data were analyzed using the software iTFlow (Cardio Flow Design Inc., Japan).

First, the region of interest was set to include the entire thoracic aorta from the aortic root to the distal end of the descending aorta (DAo) (at the level of the aortic hiatus), and the aorta was divided into 4 circumferential segments, as well as proximal and distal segments. The aortic arch (from the brachiocephalic artery bifurcation to the left subclavian artery bifurcation) was not segmented due to its short range. The circumferential segmentation of the aorta was performed by dividing the aorta into 4 equal segments (the anterior wall, posterior wall, lesser curvature, and greater curvature) based on the angle from the center of the vertical section of the aorta.

For each parameter, the area that exhibited the highest intensity distribution values during 1 cardiac cycle was examined to determine if there was a significant difference in its distribution between the EF >60% and EF <30% groups. We also examined whether there were significant intensity distribution differences among the hemodynamic parameters. Evaluation of the intensity distributions was done independently by 2 cardiovascular radiologists (T.N. and E.S.). Final decisions were reached by consensus of the 2 observers.

The EF was automatically measured using cine-MRI images.

### 2.3. Statistical analysis

The statistical analyses were carried out using JMP Pro 15 (SAS Institute Inc., Cary, NC, USA). Continuous variables are presented as mean ± standard deviation values. The Anderson-Darling test was used to evaluate whether a parameter exhibited a normal distribution, and the Levene test was used to evaluate homoscedasticity.

The Student $t$ test was used for comparisons between the 2 groups involving parameters that exhibited a normal distribution and homoscedasticity, and Welch test was used for comparisons involving heteroscedastic parameters. Wilcoxon's test was used for comparisons of parameters with non-normal distributions.

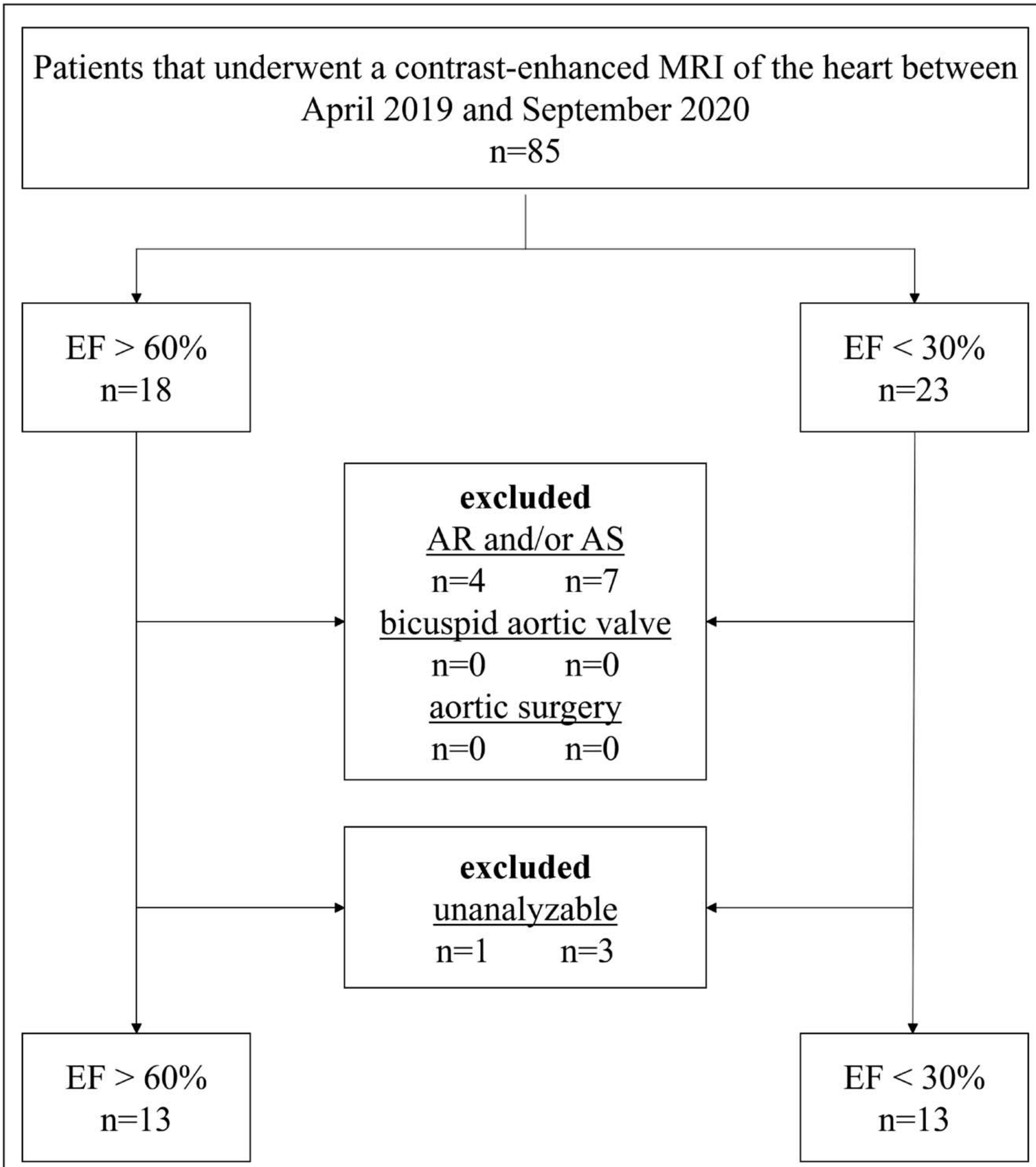


**Figure 1.** Flow chart of the inclusion and exclusion criteria. AR = aortic regurgitation, AS = aortic sclerosis, EF = ejection fraction.

Fisher exact test was used to evaluate the concordance rate between the high value areas for each pair of hemodynamic parameters (WSS-EL, WSS-Vort, and EL-Vort). The AAo and DAo were only considered to be concordant if concordance was observed in both the proximal and distal sections. Fisher exact test was also used to evaluate whether there were significant differences in the intensity distributions of the hemodynamic parameters between the AAo, arch, and/or DAo in each group. $P$ values of $<.05$ were considered statistically significant.

## 3. Results

### 3.1. The intensity distribution concordance rate

Figure 2 shows the intensity distribution patterns of WSS, EL, and Vort in a representative case.

The intensity distributions of all cases are summarized in a mosaic diagram (Table 2).

The results showed the following intensity distribution concordance rates for the EF >60% group: WSS-EL: 46.2%,

**Table 1**

**Subject demographics.**

| | EF > 60% | EF < 30% | EF > 60% vs EF < 30% *P* value |
|---|---|---|---|
| Male (%) | 38.5 | 92.3 | <.05 |
| Age (y) | 54 ± 11.6 | 49.2 ± 17.2 | .434 |
| Heart rate (bpm) | 61 ± 14.2 | 91.1 ± 21.7 | <.05 |
| Ejection fraction (%) | 67.5 ± 5.83 | 23.2 ± 2.26 | <.0001 |
| Stroke volume index (mL/min/m$^2$) | 32.5 ± 10.4 | 27.8 ± 9.84 | .268 |
| Cardiac output index (l/min/m$^2$) | 1.91 ± 0.61 | 2.39 ± 0.68 | .0828 |

Data are shown as the mean ± standard deviation.

WSS-Vort: 43.6%, and EL-Vort: 94.9%, and the following intensity distribution concordance rates for the EF <30% group: WSS-EL: 30.8%, WSS-Vort: 28.2%, and EL-Vort: 89.7%. In both groups, a significantly high concordance rate was seen between EL and Vort ($P < .001$).

### 3.2. The intensity distributions of each parameter

Figures 3–5 show mosaic diagrams of the intensity distributions for each hemodynamic parameter in each region of the thoracic aorta based on Table 2. The only significant differences between the EF groups were found in the intensity distributions of EL and Vort in the distal AAo ($P < .001$), which exhibited high values in the greater curvature in the EF >60% group and high values in the lesser curvature in the EF < 30% group.

Although there was no significant difference in the intensity distribution of WSS between the groups, among the patients with EF of <30% the intensity distribution of WSS tended to show higher values in the lesser curvature of the distal AAo, whereas in the greater curvature the values gradually tended to increase from the arch to the proximal DAo.

The high EL and Vort intensity distribution values seen in the lesser curvature from the distal AAo to the DAo in the EF <30% group.

## 4. Discussion

In this study, it was found that there was a high concordance rate between the intensity distributions of EL and Vort. It has been reported that during aortic regurgitation, regurgitation into the left ventricle causes an abnormal vortex, which increases EL in the same region, and it is expected that a correlation exists between Vort and EL.[9] The results of this study were consistent with this.

It has also been reported that in areas where the aorta is dilated, the generation of laminar flow is disturbed and turbulent flow occurs, resulting in a reduction in WSS;[10] therefore, WSS is expected to decrease in areas where Vort and EL are high. In this study, the concordance rates between the intensity distribution of WSS and those of the other 2 parameters were low, indicating, albeit indirectly, that such relationships do exist.

In the intensity distribution analysis of each parameter, the only significant differences between the EF groups were found in the intensity distributions of EL and Vort in the distal AAo, which exhibited high values in the greater curvature in the EF >60% group and high values in the lesser curvature in the EF <30% group. In the EF >60% group, the blood pumped from the heart mainly collided with the greater curvature of the AAo, causing turbulent flow in this region, which may have led to the observed increases in EL and Vort. In addition, another study found a correlation between aortic diameter expansion and EL at the level of the aortic valve.[11] Combining our findings with those of the latter study, it is suggested that in the EF >60% group the AAo may expand in the direction of the greater curvature, where EL is high. On the contrary, it is assumed that in the EF <30% group the AAo dilates toward the lesser curvature.

Fraser et al. analyzed the intensity distribution of WSS in 224 subjects with anatomically normal aortas and reported that there was a tendency for WSS at the anterior wall to be higher in the

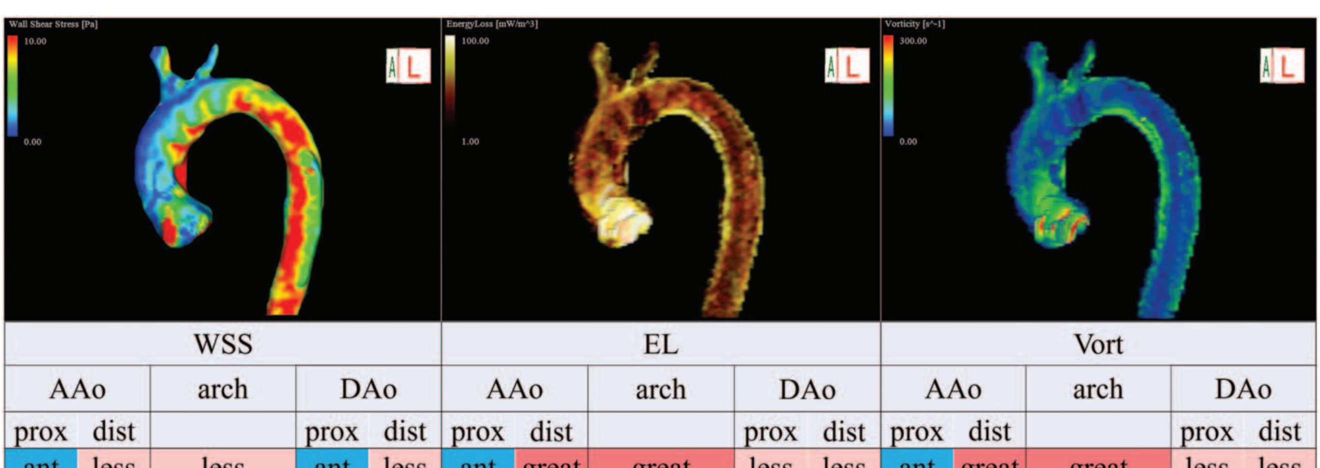


**Figure 2.** Representative case (70-year-old male, EF: >60%). AAo = ascending aorta; ant = anterior wall, DAo = descending aorta, dist = distal, EL = energy loss, great = greater curvature, less = lesser curvature, prox = proximal, Vort = vorticity WSS = wall shear stress.

**Table 2**

**Intensity distributions of WSS, EL, and Vort in the AAo, arch, and DAo.**

| | | | | AAo | | | | | | arch | | | DAo | | | | | |
|---|---|---|---|---|---|---|---|---|---|---|---|---|---|---|---|---|---|---|
| | | | | WSS | | EL | | Vort | | WSS | EL | Vort | WSS | | EL | | Vort | |
| | EF | Age | Sex | Prox | Dist | Prox | Dist | Prox | Dist | | | | Prox | Dist | Prox | Dist | Prox | Dist |
| EF > 60% | 83 | 54 | F | Post | Post | Post | Post | Post | Post | Less | Less | Less | Less | Less | Less | Less | Less | Less |
| | 77 | 62 | F | Ant | Great | Less | Great | Less | Great | Post | Less | Less | Less | Less | Less | Less | Less | Less |
| | 69 | 59 | M | Ant | Post | Great | Great | Great | Great | Ant | Less | Less | Less | Less | Ant | Ant | Ant | Ant |
| | 68 | 70 | M | Ant | Less | Ant | Great | Ant | Great | Less | Great | Great | Ant | Less | Less | Less | Less | Less |
| | 67 | 48 | F | Ant | Great | Ant | Great | Ant | Great | Less | Less | Less | Ant | Ant | Less | Less | Less | Less |
| | 67 | 58 | F | Less | Post | Less | Post | Less | Post | Great | Less | Less | Less | Less | Less | Less | Less | Less |
| | 66 | 39 | M | Less | Less | Great | Great | Great | Great | Less | Less | Less | Ant | Ant | Ant | Ant | Great | Great |
| | 65 | 46 | F | Less | Ant | Less | Great | Less | Great | Less | Less | Less | Ant | Great | Less | Less | Less | Less |
| | 65 | 69 | F | Great | Great | Great | Great | Great | Great | Less | Less | Less | Less | Less | Great | Great | Great | Great |
| | 64 | 66 | F | Less | Great | Less | Great | Less | Great | Great | Less | Less | Less | Great | Less | Less | Ant | Less |
| | 63 | 28 | M | Less | Less | Less | Less | Less | Less | Less | Less | Less | Ant | Ant | Less | Less | Less | Less |
| | 62 | 51 | F | Less | Less | Ant | Great | Ant | Great | Less | Less | Less | Less | Less | Ant | Ant | Ant | Ant |
| | 62 | 52 | M | Ant | Ant | Ant | Ant | Ant | Ant | Great | Less | Less | Great | Great | Less | Less | Less | Less |
| EF < 30% | 28 | 73 | F | Great | Less | Great | Less | Great | Less | Ant | Less | Less | Less | Less | Less | Less | Less | Less |
| | 26 | 34 | M | Ant | Great | Ant | Less | Ant | Less | Great | Less | Less | Great | Great | Less | Less | Less | Less |
| | 26 | 56 | M | Ant | Less | Ant | Less | Ant | Less | Less | Less | Less | Less | Less | Less | Less | Less | Ant |
| | 24 | 26 | M | Less | Post | Ant | Less | Ant | Less | Less | Less | Post | Less | Less | Less | Less | Less | Less |
| | 24 | 32 | M | Less | Less | Less | Less | Less | Less | Less | Less | Less | Ant | Ant | Less | Less | Less | Less |
| | 23 | 38 | M | Less | Post | Less | Less | Less | Less | Great | Less | Less | Great | Great | Less | Less | Less | Less |
| | 23 | 56 | M | Post | Less | Less | Post | Less | Post | Less | Less | Post | Less | Less | Less | Less | Less | Less |
| | 23 | 60 | M | Ant | Less | Ant | Less | Ant | Less | Ant | Less | Less | Ant | Less | Less | Less | Less | Less |
| | 22 | 35 | M | Ant | Ant | Ant | Less | Ant | Less | Ant | Less | Less | Great | Ant | Less | Less | Less | Less |
| | 21 | 33 | M | Great | Post | Ant | Less | Ant | Less | Post | Less | Less | Great | Great | Less | Less | Less | Less |
| | 21 | 46 | M | Ant | Less | Great | Ant | Great | Ant | Great | Less | Less | Great | Great | Less | Less | Less | Less |
| | 21 | 74 | M | Less | Less | Ant | Less | Ant | Less | Less | Less | Less | Less | Less | Less | Less | Less | Less |
| | 20 | 77 | M | Ant | Post | Ant | Less | Ant | Less | Great | Less | Less | Great | Ant | Less | Less | Less | Less |

AAo = ascending aorta, ant = anterior wall, DAo = descending aorta, dist = distal, EL = energy loss, great = greater curvature, less = lesser curvature, post = posterior wall, prox = proximal, Vort = vorticity, WSS = wall shear stress.

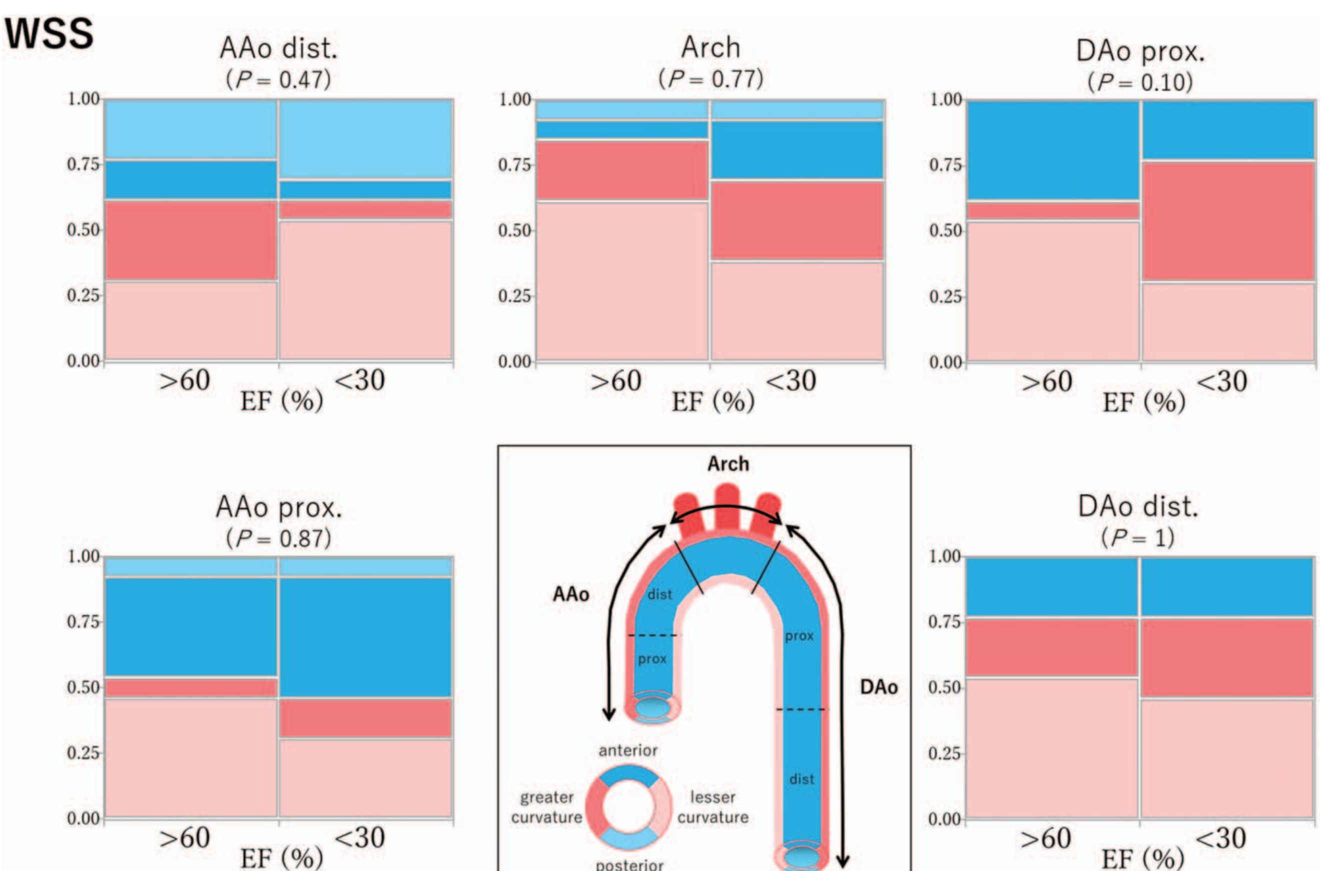


**Figure 3.** Mosaic diagrams of the intensity distributions of WSS, EL, and Vort in the AAo, arch, and DAo. Based on the results shown in Table 2, the intensity distributions of WSS (Fig. 3), EL (Fig. 4), and Vort (Fig. 5) in the AAo, arch, and DAo are shown in mosaic diagrams. Pink indicates the lesser curvature, red indicates the greater curvature, blue indicates the anterior wall, and light blue indicates the posterior wall. AAo = ascending aorta, DAo = descending aorta, dist = distal, EL = energy loss, prox = proximal, Vort = vorticity, WSS = wall shear stress.

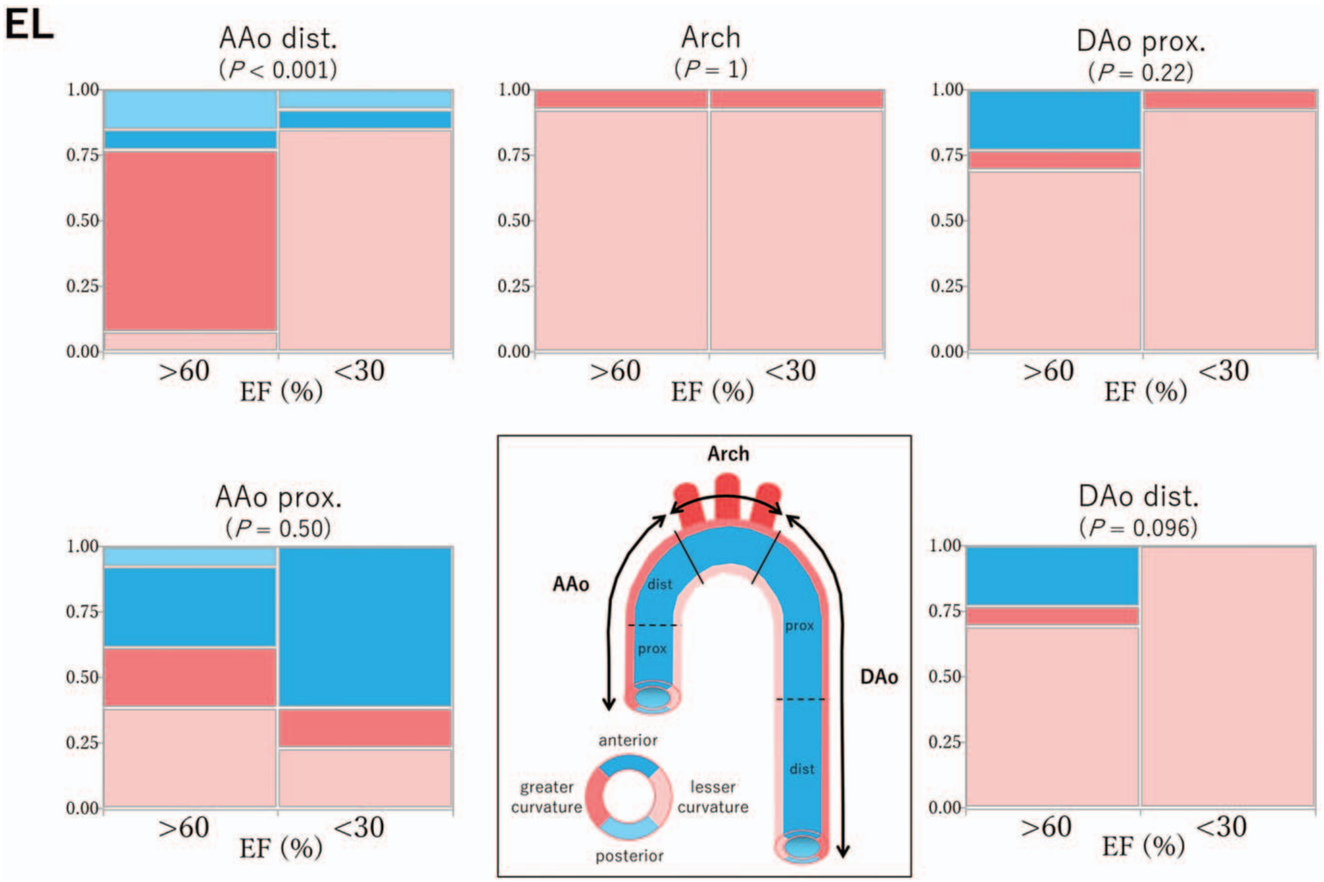


**Figure 4.** Mosaic diagrams of the intensity distributions of EL in the AAo, arch, and DAo.

section from the arch to the DAo; however, the relationship between the intensity distribution and EF was not examined.[12] In the current study, the intensity distribution of WSS in the section from the arch to the DAo exhibited higher values in the lesser curvature in the subjects with EF of >60%; however, in the proximal DAo it tended to exhibit higher values for the anterior wall, as was reported by Fraser M et al.

In the EF <30% group, the WSS intensity distribution tended to exhibit higher values in the lesser curvature of the distal AAo, whereas the values in the greater curvature gradually increased from the arch to the proximal DAo. It is presumed that in the EF <30% group the volume and velocity of the blood pumped from the heart were reduced due to decreased cardiac contractility; that is, it was difficult to maintain laminar flow. It was determined that turbulent flow was more likely to occur than laminar flow in the lesser curvature, where the direction of the vector changes particularly significantly in the section from the arch to the proximal DAo and the WSS was decreased. The high EL and Vort intensity distribution values seen in this region may also reflect this. This suggests that in patients with EF of <30%, atherosclerosis is more likely to develop in the lesser curvature of the section from the arch to the proximal DAo.

Previous study has divided the thoracic aorta into several segments and examined whether age and aortic shape affect Vort;[13] however, few studies have examined specific intensity distributions. In terms of EL, a previous study found that in patients with aortic stenosis EL was high in the section from the AAo to the anterior wall of the arch, which blood flow jets collide with;[11] however, there have been few studies involving intensity distribution analysis of normal subjects without valvular disease.

To the best of our knowledge, this is the first study about the specific intensity distributions of EL and Vort in the thoracic aorta using 4D flow MRI.

One limitation of this study was the small number of samples (13 each in the normal and reduced EF groups); therefore, it will be necessary to increase the number of samples in future studies. In this study, the relative intensity distributions of hemodynamic parameters, rather than the parameters themselves, were assessed. In the future, it will be necessary to increase the resolution of such studies as much as possible and measure the hemodynamic parameters themselves to allow them to be compared and examined in detail.

## 5. Conclusions

The intensity distributions of WSS, EL, and Vort in the thoracic aorta were examined, and significantly concordance was seen between the intensity distributions of EL and Vort. The only significant differences between the EF groups were found in the intensity distributions of EL and Vort in the distal AAo. This suggests that the distributions of atherosclerosis might depend on the EF.

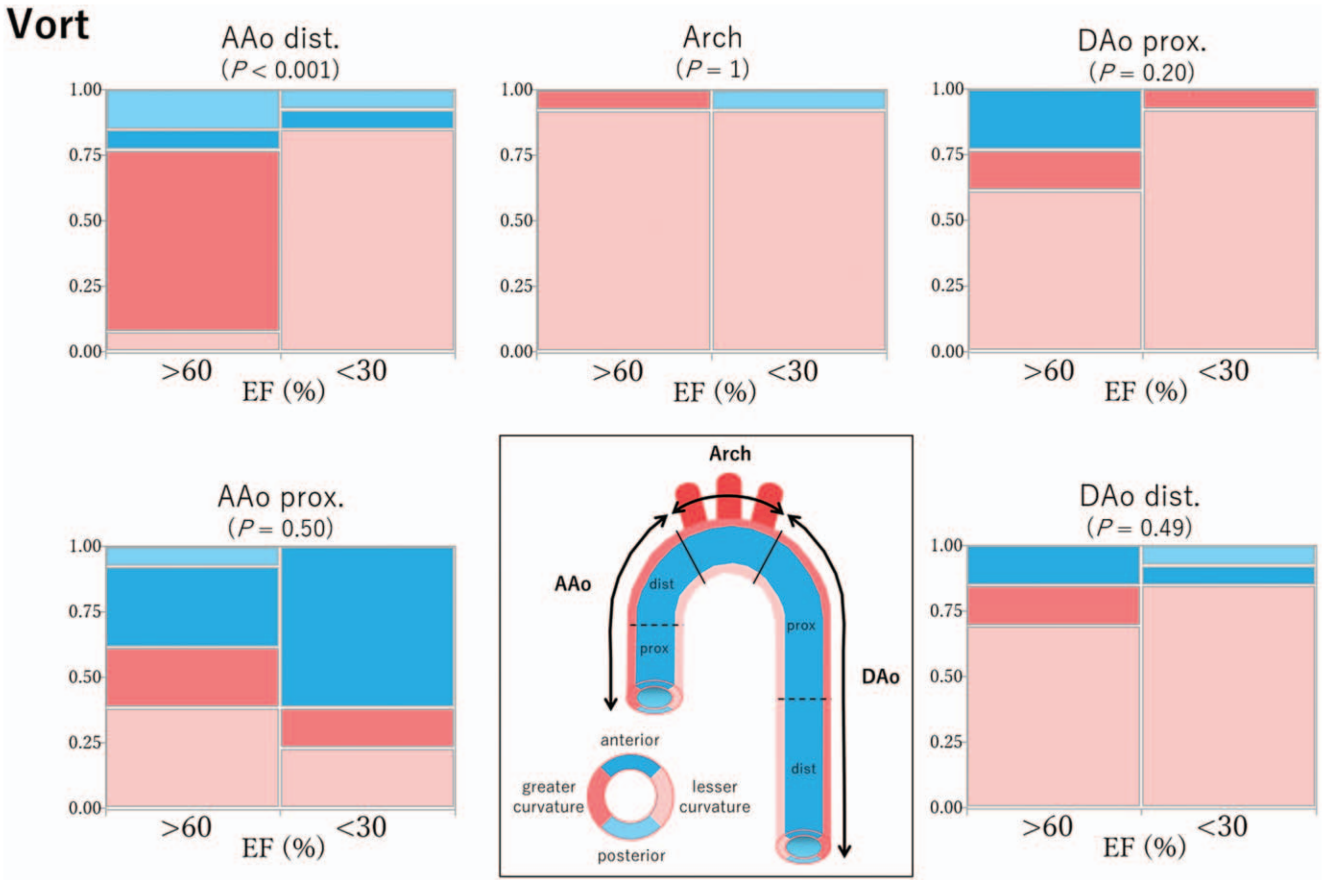


**Figure 5.** Mosaic diagrams of the intensity distributions of Vort in the AAo, arch, and DAo.

## Author contributions

**Conceptualization:** Takamasa Nishimura, Eijun Sueyoshi.
**Data curation:** Takamasa Nishimura, Eijun Sueyoshi.
**Formal analysis:** Takamasa Nishimura, Eijun Sueyoshi.
**Methodology:** Takamasa Nishimura.
**Resources:** Takamasa Nishimura.
**Writing – original draft:** Takamasa Nishimura.
**Writing – review & editing:** Eijun Sueyoshi, Hirofumi Koike, Masataka Uetani.

## References

[1] Markl M, Brendecke SM, Simon J, Barker AJ, Weiller C, Harloff A. Co-registration of the distribution of wall shear stress and 140 complex plaques of the aorta. Margn Reson Imaging 2013;31:1156–62.
[2] Fukumoto Y, Hiro T, Fujii T, et al. Localized elevation of shear stress is related to coronary plaque rupture: a 3-dimensional intravascular ultrasound study with in-vivo color mapping of shear stress distribution. J Am Coll Cardiol 2008;51:645–50.
[3] Itatani K, Miyazaki S, Furusawa T, et al. New imaging tools in cardiovascular medicine: computational fluid dynamics and 4D flow MRI. Gen Thorac Cardiovasc Surg 2017;65:611–21.
[4] Malek AM, Alper SL, Izumo S. Hemodynamic shear stress and its role in atherosclerosis. JAMA 1999;282:2035–42.
[5] Frydrychowicz A, Harloff A, Jung B, et al. Time-resolved, 3-dimensional magnetic resonance flow analysis at 3T: visualization of normal and pathological aortic vascular hemodynamics. J Comput Assist Tomogr 2007;31:9–15.
[6] Lang RM, Badano LP, Mor-Avi V, et al. Recommendations for cardiac chamber quantification by echocardiography in adults: an update from the American Society of Echocardiography and the European Association of Cardiovascular Imaging. Eur Heart J Cardiovasc Imaging 2015;16:233–70.
[7] van Ooij P, Markl M, Collins JD, et al. Aortic valve stenosis alters expression of regional aortic wall shear stress: new insights from a 4-dimensional flow magnetic resonance imaging study of 571 subjects. J Am Heart Assoc 2017;6:e005959doi: 10.1161/JAHA.117.005959.
[8] Barker AJ, Lanning C, Shandas R. Quantification of hemodynamic wall shear stress in patients with bicuspid aortic valve using phase-contrast MRI. Annals of biomedical engineering. Ann Biomed Eng 2010;38:788–800.
[9] Itatani K. When the blood flow becomes bright. Eur Heart J 2014;35:747a–52a.
[10] Takehara Y, Isoda H, Takahashi M, et al. Abnormal flow dynamics result in low wall shear stress and high oscillatory shear index in abdominal aortic dilatation: initial in vivo assessment with 4D-flow MRI. Magn Reson Med Sci 2020;19:235–46.
[11] Barker AJ, van Ooij P, Bandi K, et al. Viscous energy loss in the presence of abnormal aortic flow. Magn Reson Med 2014;72:620–8.
[12] Callaghan FM, Grieve SM. Normal patterns of thoracic aortic wall shear stress measured using four-dimensional flow MRI in a large population. Am J Physiol Heart Circ Physiol 2018;315:1174–81.
[13] Callaghan FM, Bannon P, Barin E, et al. Age-related changes of shape and flow dynamics in healthy adult aortas: a 4D flow MRI study. J Magn Reson Imaging 2018;49:90–100.